frontiers in Oncology

TYPE Original Research
PUBLISHED 06 November 2026
DOI 10.3389/fonc.2026.1976283

Check for updates

OPEN ACCESS

EDITED BY
Soumya Basu,
Dr. D. Y. Patil Biotechnology & Bioinformatics Institute, India

REVIEWED BY
Sudhir Kumar Rai,
University of Hawaii at Manoa, United States
Jennifer Sally Samson,
Sri Ramachandra Institute of Higher Education and Research, India

*CORRESPONDENCE
Yukun Fang
476796625@qq.com

†These authors have contributed equally to this work

RECEIVED 23 August 2026
REVISED 15 October 2026
ACCEPTED 15 October 2026
PUBLISHED 06 November 2026

CITATION
Zhao S, Zeng T, Liu N, Tong X, Jiao D, Chen Q and Fang Y (2026) piR-131582 suppresses lung adenocarcinoma progression by targeting USP22 and inhibiting EMT.
Front. Oncol. 16:1976283.
doi: 10.3389/fonc.2026.1976283

COPYRIGHT
© 2026 Zhao, Zeng, Liu, Tong, Jiao, Chen and Fang. This is an open-access article distributed under the terms of the Creative Commons Attribution License (CC BY). The use, distribution or reproduction in other forums is permitted, provided the original author(s) and the copyright owner(s) are credited and that the original publication in this journal is cited, in accordance with accepted academic practice. No use, distribution or reproduction is permitted which does not comply with these terms.

piR-131582 suppresses lung adenocarcinoma progression by targeting USP22 and inhibiting EMT

Shunjin Zhao[1,2†], Tianfu Zeng[3†], Ning Liu[4], Xiaoyi Tong[5], Demin Jiao[1], Qingyong Chen[1] and Yukun Fang[1*]

[1]Department of Respiratory and Critical Care Medicine, The 903rd Hospital of The PLA Joint Logistic Support Force, Hangzhou, China, [2]Department of Respiratory and Critical Care Medicine, Lanxi People's Hospital, Jinhua, China, [3]Department of Urology, Lanxi People's Hospital, Jinhua, China, [4]Fourth Department of Rehabilitation, Beidaihe Rest and Recuperation Center, Qinhuangdao, China, [5]Department of Pharmacy, Lanxi People's Hospital, Jinhua, China

Background: Piwi-interacting RNAs (piRNAs) are increasingly recognized as important regulators in tumor biology. However, which specific piRNAs actively suppress the progression and metastasis of lung adenocarcinoma (LUAD), and the mechanisms involved, remain largely undefined. This study aimed to identify tumor-suppressive piRNAs in LUAD and clarify their functional regulatory axis.
Methods: Small RNA sequencing was used to profile piRNA expression in LUAD tissues. Gain-of-function experiments were carried out by overexpressing piR-131582 in A549 and H1299 cell lines. Colony formation assays, flow cytometry, and Transwell assays were performed to evaluate cell proliferation, apoptosis, migration, and invasion, respectively. A mouse xenograft model was utilized to assess *in vivo* tumor growth. Bioinformatics prediction, combined with rescue experiments, was applied to identify and validate the downstream target of piR-131582.
Results: We found that piR-131582 was significantly downregulated in LUAD tissues. Overexpression of piR-131582 suppressed colony formation, migration, and invasion *in vitro*, while promoting apoptosis. In parallel, it notably inhibited the growth of LUAD xenograft tumors *in vivo*. Mechanistically, piR-131582 directly targeted and degraded USP22. Re-introducing USP22 effectively reversed the anti-tumor effects induced by piR-131582, restoring the epithelial-mesenchymal transition (EMT) phenotype and reactivating EMT-related signaling pathways.
Conclusions: Our results establish the piR-131582/USP22 axis as a critical tumor-suppressive node in LUAD. Restoring this natural inhibitory pathway may represent a promising direction for future therapeutic investigation in LUAD.

KEYWORDS
EMT, lung adenocarcinoma, piR-131582, Piwi-interacting RNA, USP22

Introduction

Lung cancer remains the leading cause of cancer-related death worldwide, with lung adenocarcinoma (LUAD) being the most common histological subtype (1). Over the past few years, targeted therapies and immune checkpoint inhibitors have genuinely changed the clinical landscape for a subset of patients (2, 3). However, for the majority of advanced-stage

patients, the clinical outlook remains grim. The intrinsic plasticity of LUAD cells allows them to rapidly develop therapeutic resistance and spread to distant organs (4). This clinical reality has prompted a shift in focus. Rather than simply controlling primary tumor growth, there is now a critical and unmet need to understand what naturally restrains LUAD progression and metastasis. Identifying such endogenous suppressor molecules could open entirely new avenues for lung cancer intervention.

In the search for these regulators, non-coding RNAs have emerged as important players. Piwi-interacting RNAs (piRNAs) are a class of small non-coding RNAs, typically 24 to 31 nucleotides in length. They were originally discovered for their essential role in silencing transposable elements and protecting the genomic integrity of germline cells (5). In recent years, however, the scope of piRNA biology has expanded considerably. It is now clear that piRNAs are not merely germline guardians; they are frequently dysregulated in expression and function across a wide range of somatic cancers (6). Importantly, piRNAs with opposing functions can coexist within the same tumor type. For instance, piRNA-1742 promotes renal cell carcinoma malignancy (7), whereas piR-28489 suppresses renal cell carcinoma progression by facilitating YBX-1 cytoplasm localization (8). In lung cancer, piR-651 promotes tumor formation in non-small cell lung carcinoma by upregulating cyclin D1 and CDK4 (9), and several piRNAs have been linked to patient prognosis and chemoresistance (10). These observations indicate that piRNAs are deeply involved in tumor regulation. However, a key question remains largely unanswered: which specific piRNAs actively suppress LUAD progression and metastasis, and through what molecular mechanisms do they operate?

A central process underlying LUAD metastasis is epithelial-mesenchymal transition (EMT), a fundamental developmental program that is reactivated during tumor progression. EMT drives polarized epithelial cells to lose their cell-cell junctions and acquire a highly migratory mesenchymal phenotype (11, 12). This phenotypic switch is a critical prerequisite for cancer cells to detach from the primary tumor, invade the bloodstream, and colonize distant organs (13). In recent years, accumulating evidence has suggested that piRNAs can directly regulate EMT in a variety of malignancies. For example, piRNA-31115 promotes cell proliferation and invasion via the PI3K/AKT pathway in clear cell renal carcinoma (14), and senescent neutrophil-derived exosomal piRNA-17560 promotes chemoresistance and EMT in breast cancer via FTO-mediated m6A demethylation (15). These studies indicate that piRNAs are deeply embedded in EMT regulatory networks. However, most current studies have focused on piRNAs that act as oncogenes to promote EMT. In contrast, which endogenous piRNAs are capable of actively suppressing the EMT program in LUAD, and how they achieve this mechanistically, remains poorly understood.

The execution of EMT is also heavily influenced by post-translational modifications, particularly the stability of EMT-associated proteins. Ubiquitin-specific protease 22 (USP22) is a well-known member of the deubiquitinating enzyme family. Its primary function is to remove ubiquitin tags from target proteins, thereby preventing their proteasomal degradation and stabilizing them (16). In the cancer field, USP22 is frequently characterized as an oncogene and drives tumor immune evasion and drug resistance in several types of cancer (17–19). Mechanistically, USP22 has been reported to promote EMT in pancreatic cancer and lung cancer (20, 21). Given these findings, USP22 appears to be a core node driving the acquisition of metastatic properties in LUAD. However, the endogenous regulatory mechanisms controlling USP22 remain poorly defined, and its potential post-transcriptional regulation by RNA-sparticularly piRNAs-in LUAD remains entirely unexplored.

Taken together, these gaps point to a clear research need: the identity of endogenous piRNAs that suppress LUAD metastasis, the molecular targets through which they act, and whether such a pathway can be therapeutically restored. In this study, we set out to address this need. Through small RNA sequencing of LUAD tissues, we identified piR-131582 as one of the most significantly downregulated piRNAs. We then asked whether this downregulation was functionally relevant to LUAD progression, and if so, through what molecular target it exerted its effects. Our subsequent *in vitro* and *in vivo* experiments revealed that piR-131582 functions as a critical endogenous suppressor of LUAD metastasis, and that it acts by engaging a specific oncogenic pathway that is widely implicated in EMT. Our work defines a novel piR-131582/USP22/EMT axis and suggests that restoring this natural tumor-suppressive pathway may represent a promising strategy for intervening in metastatic LUAD.

Methods and materials

Samples and small RNA sequencing

Human tissue samples were collected from patients with pathologically confirmed primary lung adenocarcinoma who underwent radical surgical resection at The 903rd Hospital of The PLA Joint Logistic Support Force. Patients with distant metastasis, multiple primary tumors, or those who had received preoperative neoadjuvant therapy were excluded. The discovery cohort used for small RNA sequencing consisted of six LUAD tumor tissues and four non-tumor lung tissues obtained from other LUAD patients. An independent cohort comprising 10 paired tumor and adjacent non-tumor tissues was used for validation. Baseline clinicopathological characteristics of the discovery cohort and the validation cohort are summarized in Supplementary Tables S1, S2, respectively. All sample collection procedures were approved by the Ethics Committee of the 903rd Hospital of the PLA Joint Logistic Support Force (approval No. 20210722/07/01/006), and written informed consent was obtained from all participants prior to sample collection.

Small RNA sequencing was performed by Yingbio Technology (Shanghai, China). In brief, total RNA was subjected to successive 3′- and 5′-adapter ligation, followed by reverse transcription. Adapter-bearing RNAs were reverse-transcribed into first-strand cDNA and amplified for library preparation. An 8% gel was applied for fragment size selection; 135–170 bp fragments were gel-isolated and purified. Library integrity was assessed using the Agilent 2100 BioAnalyzer, and single-end 50-bp sequencing was performed on the Illumina HiSeq2500 platform.

Raw reads were quality-filtered with FastQC to obtain clean reads. Clean reads of 24–32 nt, the canonical piRNA size range,

were mapped to the human genome (hg38), and reads matching rRNA, tRNA, snRNA, snoRNA, and miRNA were removed. The remaining reads were annotated against piRBase to identify piRNAs, and their expression levels were normalized to reads per million (RPM). Differentially expressed piRNAs were identified with |log2 fold change| > 1 and adjusted $P < 0.05$ (Benjamini–Hochberg correction). Detailed procedures are provided in the Supplementary Materials.

Cell lines and culture

Two human LUAD cell lines, H1299 and A549, were purchased from Kuisa Cell Biotechnology Co., Ltd. (Shanghai, China). LUAD cells were cultured in RPMI-1640 medium supplemented with 10% fetal bovine serum (FBS) and 1% penicillin-streptomycin under humidified conditions at 37 °C with 5% CO_2. Both cell lines were authenticated by short tandem repeat (STR) profiling, which confirmed that A549 and NCI-H1299 matched their respective reference profiles (100% and 98% identity, respectively). All cell lines were tested negative for mycoplasma contamination by PCR. Detailed protocols for cell culture and all cellular functional assays are provided in Supplementary Materials.

Lentivirus production

For stable overexpression or knockdown, A549 and H1299 cells were seeded in six-well plates at a density of 2×10^5 cells per well and cultured overnight. The medium was then replaced with fresh medium containing the lentiviral particles at a multiplicity of infection (MOI) of 10 in the presence of polybrene (8 μg/mL). After 24 h, the virus-containing medium was replaced with fresh complete medium, and stably transduced cells were selected with puromycin (2 μg/mL) for 72 h. Lentiviruses for piR-131582 overexpression and knockdown, together with their corresponding control vectors, were constructed as detailed in Supplementary Table S3. Lentivirus packaging was performed by Weizhen Biotechnology (Shanghai, China). Quantitative real-time reverse transcription PCR (qRT-PCR) was used to verify the efficiency of piR-131582 overexpression and knockdown.

Western blot and antibody

WB was performed to detect the expression levels of key marker proteins in LUAD cells. Detailed experimental procedures are provided in the Supplementary Materials. Primary antibodies were purchased from Abcam (Cambridge, UK), including E-cadherin (#ab40772), N-cadherin (#ab76011), Vimentin (#ab16700), USP22 (#ab195289), and TWIST (#ab50887), and snail (#ab229701). The GAPDH antibody (#2118) was obtained from Cell Signaling Technology (Danvers, MA, USA).

Flow cytometry analysis

Apoptosis was assessed by flow cytometry using an Annexin V-FITC/PI Apoptosis Detection Kit (BD Biosciences, Franklin Lakes, NJ, USA). In brief, LUAD cells were seeded in six-well plates at a density of 5×10^5 cells per well and treated with piR-131582 overexpressing or the corresponding control transfection. Cells were harvested by EDTA-free trypsinization, washed twice with cold PBS, and resuspended in 500 μL of 1× binding buffer containing 5 μL of Annexin V-FITC and 5 μL of propidium iodide (PI). After incubation for 10 min at room temperature in the dark, samples were analyzed within 1 h on a flow cytometer. Unstained and single-stained controls (Annexin V-FITC only and PI only) were used to set compensation and quadrant gates, and a minimum of 10,000 events were acquired per sample. Early apoptotic cells (Annexin V^+/PI^-) and late apoptotic/necrotic cells (Annexin V^+/PI^+) were quantified, and the total apoptotic rate was calculated as the sum of both populations. All experiments were performed with three independent biological replicates.

In vivo tumor growth

All animal procedures were conducted in accordance with the ARRIVE guidelines and relevant institutional and national regulations, and the animal study was reviewed and approved by the Ethics Committee of the 903rd Hospital of the PLA Joint Logistic Support Force (approval No. 2022-03-053).

Male BALB/c nude mice (4–5 weeks old, 16–18 g) were purchased from SLAC Laboratory Animal Co., Ltd. (Shanghai, China) and housed under specific pathogen-free conditions at 22 ± 2 °C with 50 ± 10% relative humidity under a 12-h light/dark cycle, with free access to sterilized food and water. Mice were acclimatized for one week prior to experimentation. Male mice were used to avoid potential interference from hormonal fluctuations.

For tumor induction, 5×10^6 lentivirus-transduced A549 cells suspended in 100 μL of serum-free medium were injected subcutaneously into the right dorsal flank of each mouse. One week after inoculation, tumor dimensions were measured with a digital caliper, and tumor volume was calculated using the formula $V = (\text{length} \times \text{width}^2)/2$. Mice bearing tumors with a volume ≥ 40 mm^3 were stratified by tumor volume and randomly allocated into two groups (n = 4 per group), the piR-131582-overexpressing group and the empty vector control (NC) group, using a computer-generated random sequence. Mice that failed to reach this threshold were excluded from the study. Tumor volumes were measured every 2–3 days by an investigator blinded to group allocation. After the 30-day observation period, mice were euthanized by cervical dislocation under deep isoflurane anesthesia, and tumor xenografts were excised, weighed, photographed, and processed for further analyses. Mice were monitored daily and euthanized early if a tumor exceeded 2,000 mm^3 or if body weight fell by more than 20%. Body weights did not differ significantly between groups, and no signs of systemic toxicity were observed.

Statistical analysis

Data are presented as the mean ± SD from at least three independent biological replicates. Comparisons between two groups were performed using a two-tailed Student's t-test or the Wilcoxon test. Comparisons among multiple groups were performed using one-way ANOVA followed by Tukey's *post-hoc* test.

Tumor growth curves were analyzed by repeated-measures ANOVA. A P value below 0.05 was considered statistically significant. Statistical analyses were performed using GraphPad Prism (v8.0.1) and R (v4.5.2).

Results

piR-131582 is downregulated in LUAD tissues

To search for potential tumor-suppressive piRNAs in LUAD, we performed small RNA sequencing on tumor tissues and non-tumor tissues. Comparative analysis revealed a set of piRNAs that were significantly differentially expressed between the two groups (Figure 1A). Among these, piR-131582 was identified as one of the most prominently downregulated piRNAs in the LUAD cohort (Figure 1B). The downregulation of piR-131582 was further confirmed by qRT-PCR in 10 paired tumor and adjacent non-tumor tissues (Supplementary Figure S1). Given that the downregulation of regulatory RNAs often implies the loss of their protective functions, we hypothesized that piR-131582 might act as a tumor suppressor in LUAD. This downregulation aligns with recent reports showing that specific piRNAs are silenced during lung tumorigenesis (10). Based on this, we selected piR-131582 for subsequent functional and mechanistic studies. piR-131582 corresponds to piR-hsa-131582 in piRBase, a 26-nt piRNA located on chromosome 21 at positions 8441146 to 8441171 (plus strand), with the mature sequence CGCGACCTCAGATCAGACGTGCCGAC (Supplementary Table S4).

Overexpression of piR-131582 inhibits LUAD cell proliferation and promotes apoptosis

To explore the biological function of piR-131582, we first examined its basal expression levels in LUAD cell lines. As shown in Figure 2A, piR-131582 was significantly downregulated in A549 and H1299 cells compared with the normal bronchial epithelial cell line BEAS-2B. We then constructed the knockdown and overexpression lentiviral vectors and transduced them into A549 and H1299 cells. The transduced cells showed significant differential expression of piR-131582 (Supplementary Figure S2). Colony formation assays showed that the number of colonies formed by piR-131582-overexpressing cells was significantly reduced compared with the negative control (NC) groups (Figure 2B, $P < 0.001$). Flow cytometry analysis using Annexin V/PI staining indicated that the proportion of apoptotic cells was markedly increased upon piR-131582 overexpression (Figure 2C, $P < 0.001$). Collectively, these data suggest that piR-131582 plays a positive role in suppressing LUAD cell survival and clonogenic capacity.

piR-131582 inhibits migration, invasion, and EMT in LUAD cells

Metastasis is a major factor contributing to LUAD mortality. To evaluate the impact of piR-131582 on cell motility, we performed Transwell assays. The results showed that overexpression of piR-131582 dramatically reduced the number of migrating and invading cells in both A549 and H1299 cell lines (Figure 3A, all $P < 0.001$). To further confirm this phenotype through a loss-of-function approach, we knocked down endogenous piR-131582 using a specific shRNA (sh-piR-131582) in both cell lines. As expected, silencing

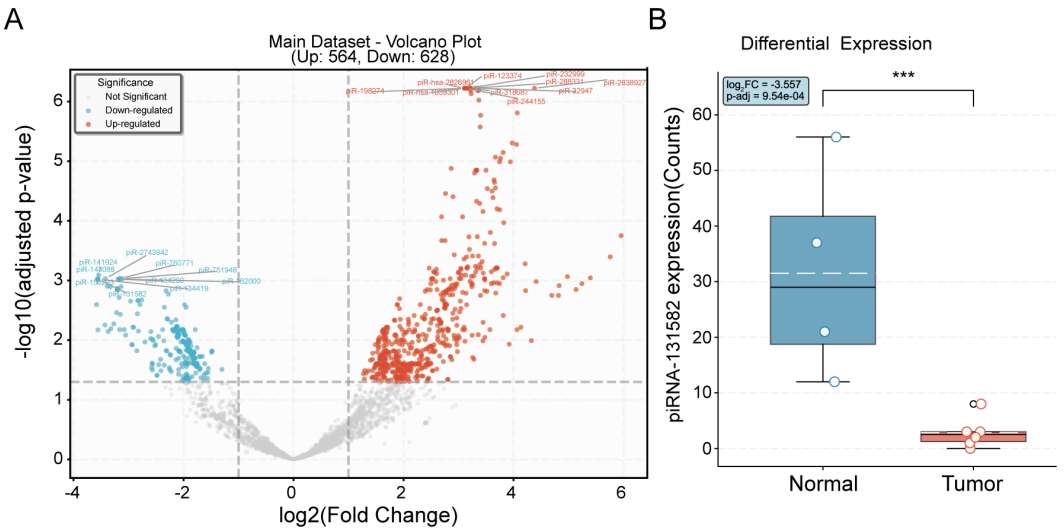


FIGURE 1
Identification of piR-131582 as a downregulated piRNA in LUAD. **(A)** Volcano plot of differentially expressed piRNAs between six LUAD tumor tissues and four non-tumor tissues. Up-regulated and down-regulated piRNAs are indicated, and piR-131582 is highlighted. **(B)** Differential expression of piR-131582 between LUAD tumor tissues and non-tumor tissues from small RNA sequencing. Data are presented as mean ± SD. ***P < 0.001 by Student's t-test.

10.3389/fonc.2026.1976283

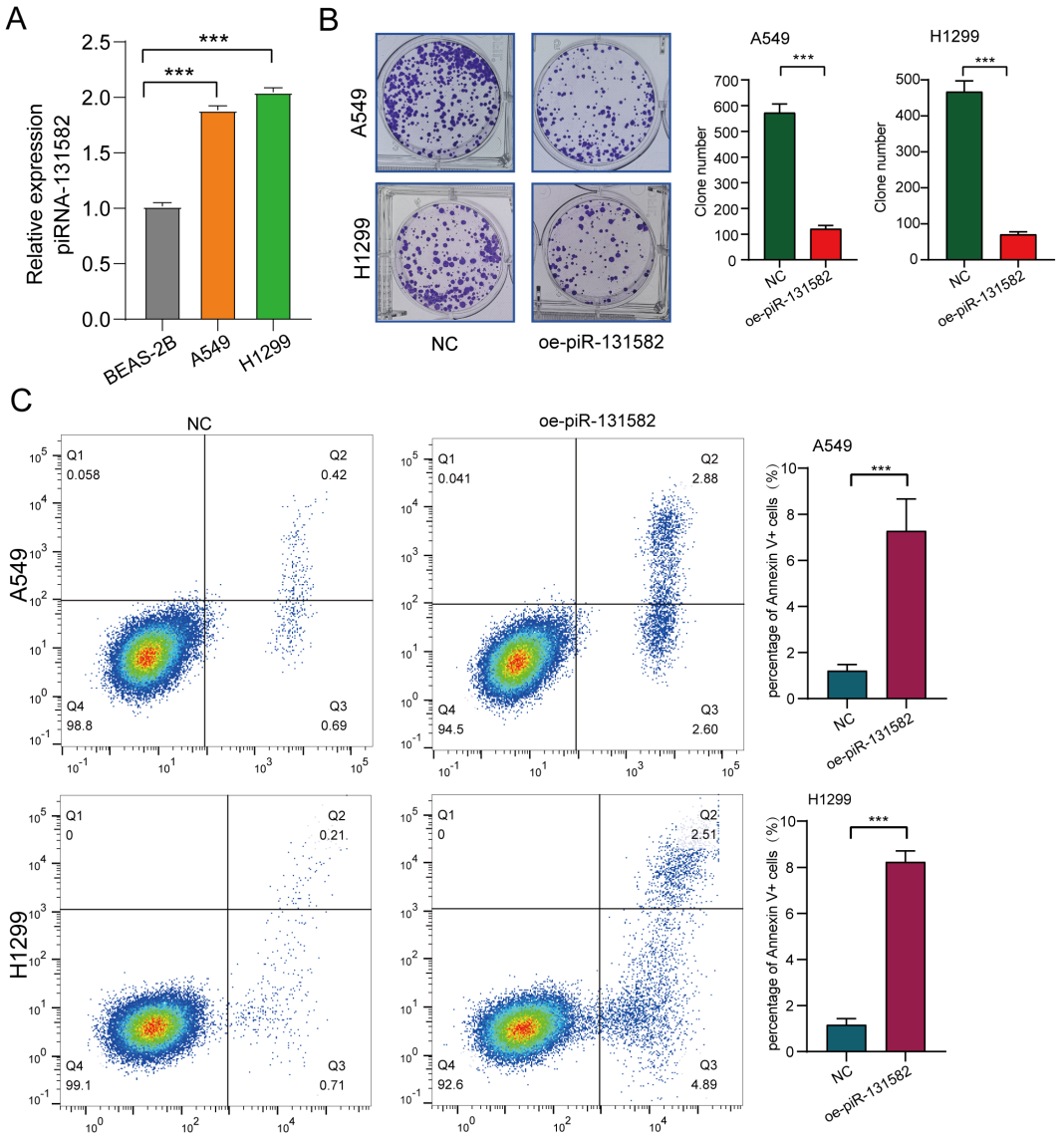


FIGURE 2
Overexpression of piR-131582 suppresses LUAD cell proliferation and promotes apoptosis. **(A)** Relative piR-131582 expression in the normal bronchial epithelial cell line BEAS-2B and the LUAD cell lines A549 and H1299. **(B)** Representative images and quantification of colony-formation assays in A549 and H1299 cells with piR-131582 overexpression (oe-piR-131582) or control (NC) transduction. **(C)** Flow-cytometry analysis of apoptosis by Annexin V/PI staining, with representative scatter plots and quantification of Annexin V-positive cells. Data are presented as mean ± SD (n = 3). ***P < 0.001 by Student's t-test.

piR-131582 significantly enhanced the migratory and invasive capacities of A549 and H1299 cells compared with the NC group (Supplementary Figure S3, all P < 0.001). Given that EMT is a critical step for metastasis, we next examined the expression of EMT-related proteins. WB results indicated that piR-131582 overexpression upregulated the epithelial marker E-cadherin, while concurrently downregulating the mesenchymal markers N-cadherin and Vimentin (Figure 3C). These findings indicate that piR-131582 effectively inhibits EMT in LUAD cells.

USP22 is a downstream target of piR-131582

To decipher the molecular mechanism underlying the anti-EMT effect of piR-131582, we performed bioinformatic target prediction. Among the candidate targets, USP22 caught our attention because it has been previously reported to promote EMT and metastasis in various cancers (20, 21). As shown in Figure 4A, the prediction algorithm suggested a direct binding site between piR-131582 and the 3'-UTR of USP22 mRNA. To validate this interaction, we examined USP22 protein levels following piR-131582 overexpression. WB analysis confirmed that overexpression of piR-131582 significantly suppressed USP22 protein expression in both A549 and H1299 cells (Figure 4B). PCR analysis further showed that USP22 mRNA levels were significantly reduced upon piR-131582 overexpression in both A549 and H1299 cells (Supplementary Figure S4). These results establish USP22 as a crucial downstream target that is degraded by piR-131582 in LUAD cells. To further validate the association of piR-131582 and USP22 mRNA with the PIWI complex, we performed an

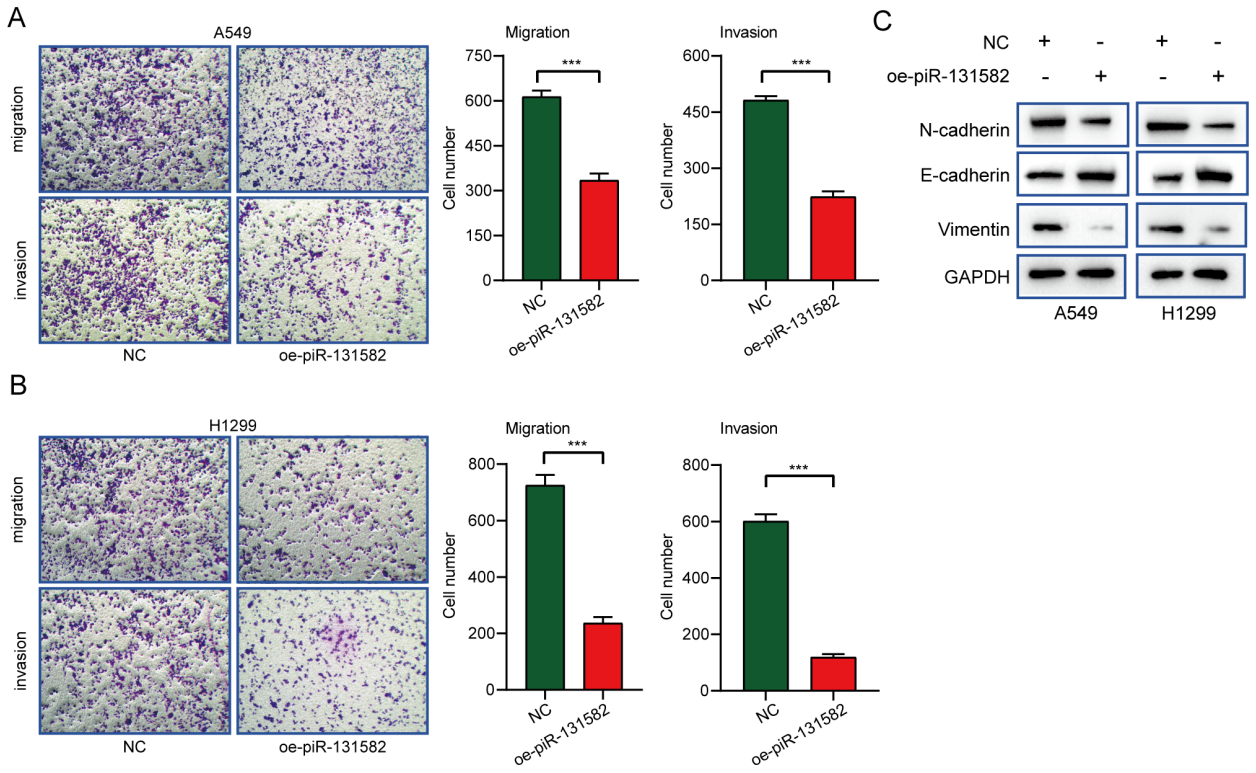


FIGURE 3
piR-131582 inhibits migration, invasion, and EMT in LUAD cells. **(A, B)** Representative images and quantification of Transwell migration and invasion assays in A549 **(A)** and H1299 **(B)** cells with piR-131582 overexpression (oe) or control (NC). **(C)** Western blot analysis of E-cadherin, N-cadherin, and Vimentin. GAPDH served as the loading control. Data are presented as mean ± SD (n = 3). ***P < 0.001 by Student's t-test.

RNA immunoprecipitation (RIP) assay using an anti-PIWI antibody. The results showed that both piR-131582 and USP22 mRNA were significantly enriched in the PIWI immunoprecipitates compared with the IgG control (Figure 4C, both P < 0.01), confirming that piR-131582 physically associates with USP22 mRNA in a PIWI-dependent manner. These results establish USP22 as a crucial downstream target that is negatively regulated by piR-131582 in LUAD cells.

To further confirm this regulatory relationship *in vivo*, A549 cells stably overexpressing piR-131582 or the control vector were implanted subcutaneously into nude mice. Tumors in the piR-131582 overexpressing group were significantly smaller in both volume and final weight than those in the NC group (Figures 4D, E). Body weights remained similar between the two groups, and neither group showed signs of toxicity. Immunohistochemistry of the harvested tumors showed reduced USP22 and the mesenchymal marker N-cadherin and increased cleaved caspase-3 in the piR-131582-overexpressing group (Figure 4F), consistent with the *in vitro* EMT changes. Together, these results indicate that piR-131582 suppresses USP22 and the EMT phenotype *in vivo*.

USP22 overexpression partially reverses the anti-tumor effects of piR-131582

To prove that the tumor-suppressive function of piR-131582 is mediated through USP22, we performed rescue experiments. We co-transfected A549 and H1299 cells with piR-131582 and USP22 overexpression plasmid. Notably, USP22 partially reversed the inhibitory effects of piR-131582 on migration, invasion (Figure 5A), and colony formation (Figure 5B). At the molecular level, while piR-131582 suppressed the mesenchymal phenotype, adding back USP22 restored the expression of mesenchymal markers and transcription factors, including N-cadherin, Vimentin, Snail, and Twist (Figure 5C). Collectively, these rescue experiments demonstrate that piR-131582 suppresses LUAD progression and metastasis primarily through the targeted degradation of USP22 and the subsequent inhibition of EMT.

Binding of piR-131582 to the USP22 3′-UTR is required for its tumor-suppressive function

While the rescue experiments above suggest that USP22 is a key downstream mediator of piR-131582, they do not formally prove that piR-131582 directly binds to USP22. To address this, we first examined the predicted interaction site. As shown in Figure 6A, the piR-131582 sequence contains a complementary binding region within the 3'-UTR of USP22 mRNA (Figure 6A). To test whether this specific site mediates the regulatory effect, we performed dual-luciferase reporter assays using constructs containing either the wild-type (wt) or a mutated (mut) binding site (Figure 6B). Overexpression of piR-131582 significantly reduced the luciferase activity of the USP22-WT construct, whereas it had no significant effect on the USP22-MUT construct (Figure 6C, P<0.05).

10.3389/fonc.2026.1976283

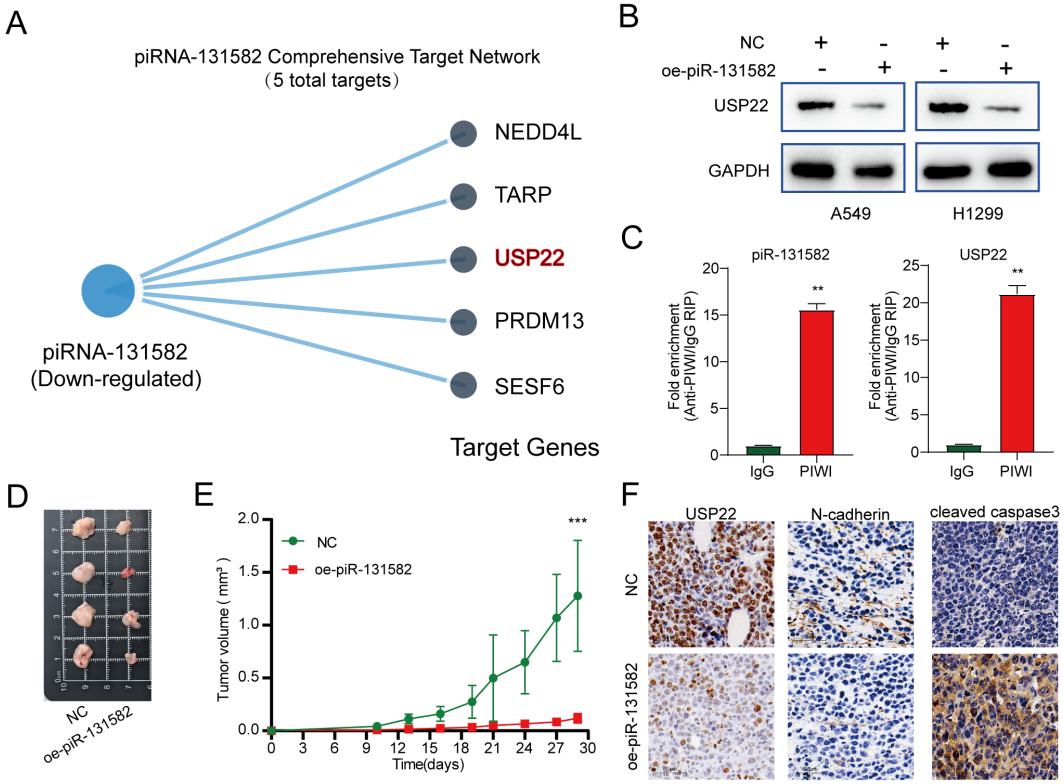


FIGURE 4
piR-131582 targets USP22 and suppresses tumor growth *in vivo*. **(A)** Predicted regulatory network of piR-131582 target genes. **(B)** Western blot analysis of USP22 in A549 and H1299 cells with piR-131582 overexpression (oe) or control (NC). GAPDH served as the loading control. **(C)** PIWI RNA immunoprecipitation (RIP) showing enrichment of piR-131582 and USP22 mRNA in the anti-PIWI immunoprecipitate relative to IgG. **P < 0.01. **(D, E)** Representative tumors **(D)** and tumor volume **(E)** of xenografts formed by A549 cells with piR-131582 overexpression (oe-piR-131582) or control (NC) (n = 4 per group). **(F)** Immunohistochemistry for USP22, N-cadherin, and cleaved caspase-3 in xenograft tumors. Data are presented as mean ± SD. **P < 0.01, ***P < 0.001 by Student's t-test.

Conversely, silencing piR-131582 enhanced the luciferase activity of the WT construct but not the MUT construct (Figure 6C). These results confirm that piR-131582 binds to the predicted site within the USP22 3'-UTR.

To further establish that this binding site is functionally relevant, we performed rescue experiments using wt- or mut- USP22 constructs. As shown in Figure 6D, overexpression of wt-USP22 alone promoted cell migration and invasion. However, when wt-USP22 was co-overexpressed with piR-131582, its pro-migratory and pro-invasive effects were significantly reversed, consistent with piR-131582-mediated degradation of wt-USP22. In contrast, when mut-USP22, which lacks the piR-131582 binding site, was co-overexpressed with piR-131582, the pro-migratory and pro-invasive effects were preserved as the mutated 3'-UTR rendered USP22 resistant to piR-131582-mediated degradation (Figure 6D). Collectively, these data provide direct evidence that piR-131582 suppresses LUAD progression by specifically targeting the 3'-UTR of USP22 and promoting its degradation.

Discussion

The present study characterizes piR-131582 as a novel tumor suppressor in lung adenocarcinoma. Mechanistically, we established a pathway in which piR-131582 directly binds to the 3'-UTR of USP22 mRNA and promotes its degradation, thereby blocking USP22-driven EMT. This work extends our current understanding of piRNA biology in cancer (6). The discovery of piR-131582 downregulation in LUAD adds to the growing list of piRNAs that are silenced during malignant transformation. Given its tissue-specific profile, piR-131582 holds promise as an emerging biomarker for early lung cancer detection or intervention.

Our data provide several lines of evidence supporting the direct regulation of USP22 by piR-131582. First, bioinformatic prediction identified a complementary binding site within the USP22 3'-UTR. Second, the PIWI-RIP assay confirmed that both piR-131582 and USP22 mRNA are physically enriched in the PIWI immunoprecipitate, indicating that they associate within a piRNA-induced silencing complex (piRISC) (22). Third, dual-luciferase reporter assays showed that piR-131582 significantly suppressed the activity of the wild-type USP22 3'-UTR but had no effect on a construct carrying a mutated binding site. Fourth, rescue experiments using the binding-site-mutant USP22 demonstrated that the pro-migratory and pro-invasive effects of USP22 were preserved in the presence of piR-131582, whereas wt-USP22 was degraded. Together, these findings provide direct evidence that piR-131582 targets USP22 through a specific 3'-UTR interaction, rather than through an indirect mechanism.

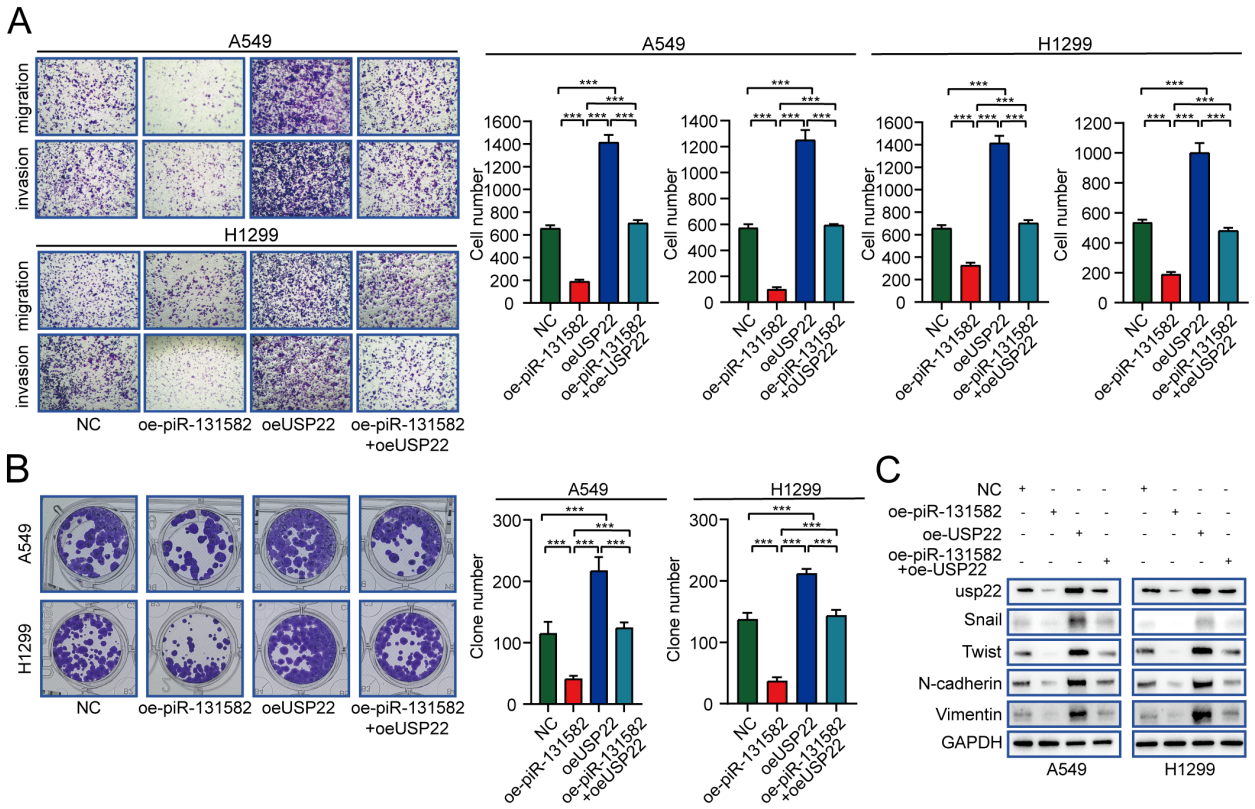


FIGURE 5
USP22 overexpression reverses the anti-tumor effects of piR-131582. **(A, B)** Transwell migration and invasion **(A)** and colony-formation **(B)** assays in A549 and H1299 cells expressing control (NC), piR-131582 overexpression (oe-piR-131582), USP22 overexpression (oeUSP22), or oe-piR-131582 combined with oeUSP22. **(C)** Western blot analysis of USP22, Snail, Twist, N-cadherin, and Vimentin under the indicated conditions. Data are presented as mean ± SD (n = 3). ***P < 0.001 by one-way ANOVA with Tukey's post-hoc test.

USP22 is a well-known deubiquitinating enzyme that regulates protein stability by removing ubiquitin chains (16). In our study, we found that USP22 is stably expressed in LUAD cells, and this is largely due to the downregulation of piR-131582. This finding is consistent with earlier reports that USP22 promotes the progression of various cancers, including NSCLC and gastric cancer (21, 23). The key observation from our rescue experiments is that overexpression of USP22 was sufficient to partially counteract the anti-tumor effects of piR-131582, and the binding-site-mutant USP22 fully restored the migratory phenotype. This provides strong evidence that USP22 is the critical effector protein downstream of piR-131582 in this specific context.

The most clinically relevant aspect of our study is the link between the piR-131582/USP22 axis and EMT. Previous studies have suggested that USP22 induces EMT by stabilizing Snail or activating the PI3K/AKT pathway (24, 25). Our data fit neatly into this model: when piR-131582 is present, it acts as a brake on USP22, keeping EMT in check. However, the downregulation of piR-131582 in LUAD removes this brake, leading to USP22 accumulation, subsequent EMT activation, and ultimately a more aggressive metastatic phenotype. Importantly, our *in vivo* IHC analysis confirmed that piR-131582 overexpression reduced USP22 and N-cadherin expression while increasing cleaved caspase-3 in xenograft tumors, further supporting the functional relevance of this axis in a physiological context. This highlights a potential therapeutic strategy. Although directly inhibiting USP22 with small molecules is currently challenging due to the conserved nature of deubiquitinase active sites (26), whether nanoparticle-based delivery of piR-131582 can achieve therapeutic benefit remains an important future direction requiring dedicated treatment and metastasis models (27).

Several limitations of this work should be noted. First, while our *in vitro* and murine xenograft data are compelling, validation in larger clinical cohorts is still needed to determine whether piR-131582 levels correlate with patient survival or treatment response. Second, USP22 is a multifunctional protein; beyond EMT, it is also involved in cell cycle regulation and autophagy (28, 29). Although our rescue experiments strongly highlight the importance of EMT, we cannot completely exclude the contributions of these alternative pathways. Third, while our luciferase and mutant rescue assays confirm the functional importance of the predicted binding site, the precise stoichiometry and kinetics of the piR-131582/USP22

10.3389/fonc.2026.1976283

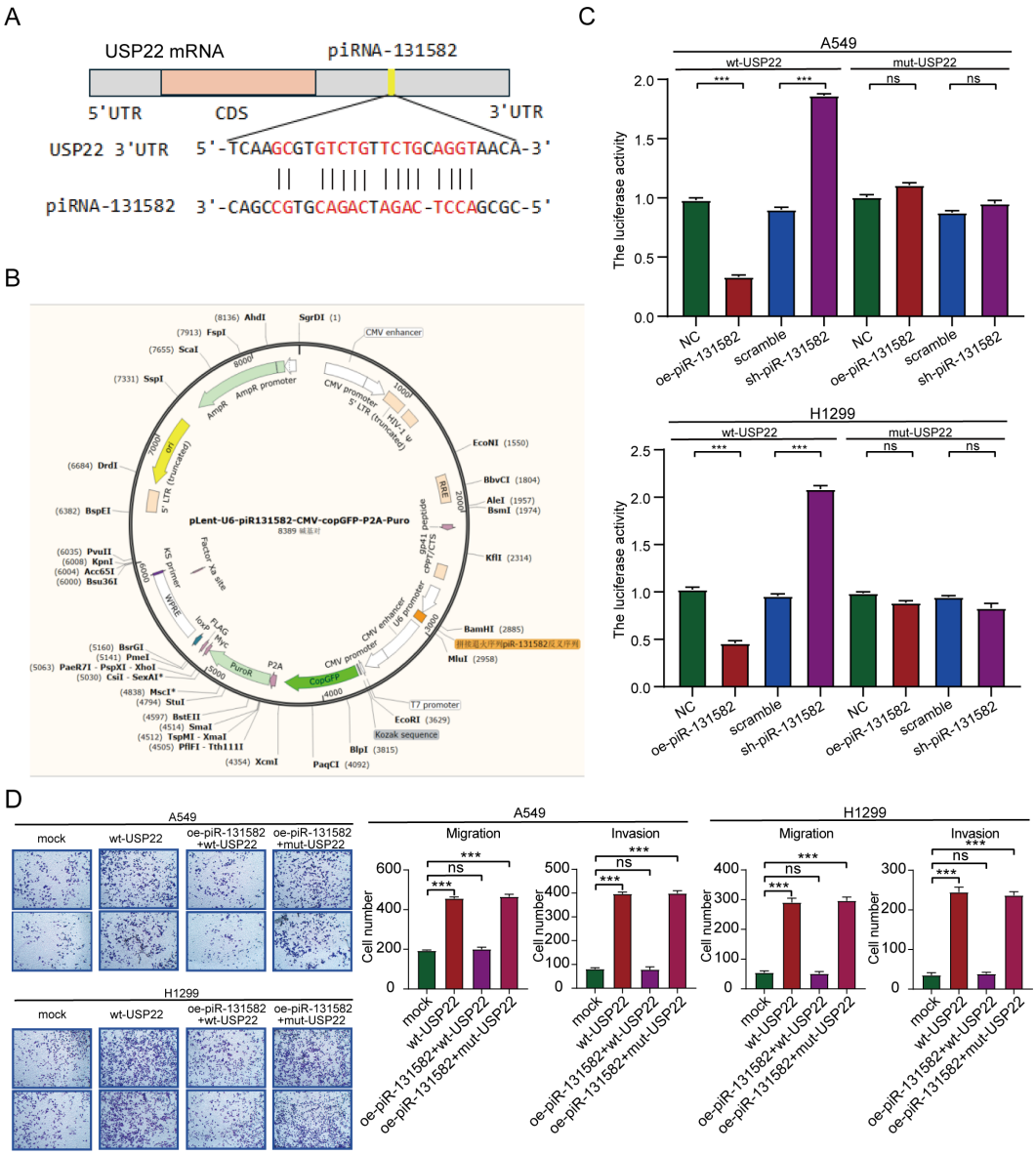


FIGURE 6
piR-131582 directly binds the USP22 3′-UTR through a specific site. **(A)** Predicted complementary binding between piR-131582 and the 3′-UTR of USP22 mRNA. **(B)** Schematic of the wild-type (USP22-WT) and binding-site-mutated (USP22-MUT) luciferase reporter constructs. **(C)** Dual-luciferase reporter assay in A549 and H1299 cells with piR-131582 overexpression (oe-piR-131582) or knockdown (sh-piR-131582), using the USP22-WT or USP22-MUT reporter. **(D)** Transwell migration and invasion assays with Mock, WT-USP22, oe-piR-131582 plus WT-USP22, or oe-piR-131582 plus mutant USP22 (mut-USP22). Data are presented as mean ± SD (n = 3). ***P < 0.001, ns not significant by one-way ANOVA with Tukey's post-hoc test

interaction remain to be determined. Future studies utilizing USP22-specific inhibitors or clinical samples are required to translate these findings into clinical practice.

Conclusions

In summary, our study reveals a novel tumor-suppressive mechanism in lung adenocarcinoma, in which piR-131582 directly degrades USP22, thereby inhibiting EMT. These findings not only deepen our understanding of piRNA-driven LUAD suppression but also provide a rationale for future investigation of whether restoring piR-131582 can be exploited therapeutically.

Data availability statement

The raw small RNA sequencing data generated for this study have been deposited in the NCBI Sequence Read Archive (SRA) under the accession number [PRJNA1541646].

Ethics statement

The studies involving humans were approved by The Ethics Committee of The 903rd Hospital of PLA Joint Logistic Support Force. The studies were conducted in accordance with the local

legislation and institutional requirements. The participants provided their written informed consent to participate in this study. The animal study was approved by The Ethics Committee of The 903rd Hospital of PLA Joint Logistic Support Force. The study was conducted in accordance with the local legislation and institutional requirements.

Author contributions

SZ: Conceptualization, Writing – original draft, Data curation. TZ: Formal analysis, Visualization, Writing – review & editing. NL: Project administration, Writing – review & editing. XT: Formal analysis, Visualization, Writing – original draft. DJ: Investigation, Writing – original draft. QC: Supervision, Writing – review & editing. YF: Conceptualization, Writing – review & editing, Writing – original draft.

Funding

The author(s) declared that financial support was received for this work and/or its publication. This study was supported by the Zhejiang Provincial Medical and Health Science and Technology Development Program (Project No. 2024KY505) and the Zhejiang Provincial Medical and Health Science and Technology Development Program (Grant No. 2023KY207).

Acknowledgments

Jie Yan provided the resources in the study.

Conflict of interest

The author(s) declared that this work was conducted in the absence of any commercial or financial relationships that could be construed as a potential conflict of interest.

Generative AI statement

The author(s) declared that generative AI was not used in the creation of this manuscript.

Any alternative text (alt text) provided alongside figures in this article has been generated by Frontiers with the support of artificial intelligence and reasonable efforts have been made to ensure accuracy, including review by the authors wherever possible. If you identify any issues, please contact us.

Publisher's note

All claims expressed in this article are solely those of the authors and do not necessarily represent those of their affiliated organizations, or those of the publisher, the editors and the reviewers. Any product that may be evaluated in this article, or claim that may be made by its manufacturer, is not guaranteed or endorsed by the publisher.

Supplementary material

The Supplementary Material for this article can be found online at: https://www.frontiersin.org/articles/10.3389/fonc.2026.1976283/full#supplementary-material

References

1. Siegel RL, Kratzer TB, Wagle NS, Sung H, Jemal A. Cancer statistics, 2026. *CA Cancer J Clin*. (2026) 76:e70043. doi: 10.3322/caac.70043

2. Herbst RS, Morgensztern D, Boshoff C. The biology and management of non-small cell lung cancer. *Nature*. (2018) 553:446–54. doi: 10.1038/nature25183

3. Zulfiqar B, Farooq A, Kanwal S, Asghar K. Immunotherapy and targeted therapy for lung cancer: Current status and future perspectives. *Front Pharmacol*. (2022) 13:1035171. doi: 10.3389/fphar.2022.1035171

4. Burns TF, Dacic S, Chakka A, Miller E, Velez MA, Somasundaram A, et al. MET alterations are enriched in lung adenocarcinoma brain metastases, defining a distinct biologic subtype. *J Clin Invest*. (2025) 136:e194708. doi: 10.1172/JCI194708

5. Aravin AA, Sachidanandam R, Girard A, Fejes-Toth K, Hannon GJ. Developmentally regulated piRNA clusters implicate MILI in transposon control. *Science*. (2007) 316:744–7. doi: 10.1126/science.1142612

6. Liu Y, Dou M, Song X, Dong Y, Liu S, Liu H, et al. The emerging role of the piRNA/piwi complex in cancer. *Mol Cancer*. (2019) 18:123. doi: 10.1186/s12943-019-1052-9

7. Zhang W, Zheng Z, Wang K, Mao W, Li X, Wang G, et al. piRNA-1742 promotes renal cell carcinoma malignancy by regulating USP8 stability through binding to hnRNPU and thereby inhibiting MUC12 ubiquitination. *Exp Mol Med*. (2023) 55:1258–71. doi: 10.1038/s12276-023-01010-3

8. Wang R, Li F, Lin Y, Lu Z, Luo W, Xu Z, et al. piR-RCC suppresses renal cell carcinoma progression by facilitating YBX-1 cytoplasm localization. *Adv Sci (Weinh)*. (2025) 12:e14398. doi: 10.1002/advs.202414398

9. Li D, Luo Y, Gao Y, Yang Y, Wang Y, Xu Y, et al. piR-651 promotes tumor formation in non-small cell lung carcinoma through the upregulation of cyclin D1 and CDK4. *Int J Mol Med*. (2016) 38:927–36. doi: 10.3892/ijmm.2016.2671

10. Song L, Zhou JG, Ma H. The potential role of PIWI-interacting RNAs in non-small cell lung cancer. *Front Oncol*. (2025) 15:1660236. doi: 10.3389/fonc.2025.1660236

11. Thiery JP, Acloque H, Huang RY, Nieto MA. Epithelial-mesenchymal transitions in development and disease. *Cell*. (2009) 139:871–90. doi: 10.1016/j.cell.2009.11.007

12. Brabletz T, Kalluri R, Nieto MA, Weinberg RA. EMT in cancer. *Nat Rev Cancer*. (2018) 18:128–34. doi: 10.1038/nrc.2017.118

13. De Craene B, Berx G. Regulatory networks defining EMT during cancer initiation and progression. *Nat Rev Cancer*. (2013) 13:97–110. doi: 10.1038/nrc3447

14. Du X, Li H, Xie X, Shi L, Wu F, Li G, et al. piRNA-31115 promotes cell proliferation and invasion via PI3K/AKT pathway in clear cell renal carcinoma. *Dis Markers*. (2021) 2021:6915329. doi: 10.1155/2021/6915329

15. Ou B, Liu Y, Gao Z, Xu J, Yan Y, Li Y, et al. Senescent neutrophils-derived exosomal piRNA-17560 promotes chemoresistance and EMT of breast cancer via FTO-mediated m6A demethylation. *Cell Death Dis*. (2022) 13:905. doi: 10.1038/s41419-022-05317-3

16. Nijman SM, Luna-Vargas MP, Velds A, Brummelkamp TR, Dirac AM, Sixma TK, et al. A genomic and functional inventory of deubiquitinating enzymes. *Cell*. (2005) 123:773–86. doi: 10.1016/j.cell.2005.11.007

17. Liu K, Iyer R, Li Y, Zhu J, Cai Z, Wei J, et al. USP22 drives tumor immune evasion and checkpoint blockade resistance through EZH2-mediated epigenetic silencing of MHC-I. *J Clin Invest*. (2025) 136:e193162. doi: 10.1172/JCI193162

18. Shan Q, Yin L, Zhan Q, Yu J, Pan S, Zhuo J, et al. The p-MYH9/USP22/HIF-1α axis promotes lenvatinib resistance and cancer stemness in hepatocellular carcinoma. *Signal Transduct Target Ther*. (2024) 9:249. doi: 10.1038/s41392-024-01963-5

19. Zeng K, Xie W, Wang C, Wang S, Liu W, Su Y, et al. USP22 upregulates ZEB1-mediated VEGFA transcription in hepatocellular carcinoma. *Cell Death Dis*. (2023) 14:194. doi: 10.1038/s41419-023-05699-y

20. Ning Z, Wang A, Liang J, Xie Y, Liu J, Yan Q, et al. USP22 promotes epithelial-mesenchymal transition via the FAK pathway in pancreatic cancer cells. *Oncol Rep*. (2014) 32:1451–8. doi: 10.3892/or.2014.3354

21. Hu J, Yang D, Zhang H, Liu W, Zhao Y, Lu H, et al. USP22 promotes tumor progression and induces epithelial-mesenchymal transition in lung adenocarcinoma. *Lung Cancer*. (2015) 88:239–45. doi: 10.1016/j.lungcan.2015.02.019

22. Siomi MC, Sato K, Pezic D, Aravin AA. PIWI-interacting small RNAs: The vanguard of genome defence. *Nat Rev Mol Cell Biol*. (2011) 12:246–58. doi: 10.1038/nrm3081

23. Ma Y, Fu HL, Wang Z, Huang H, Ni J, Song J, et al. USP22 maintains gastric cancer stem cell stemness and promotes gastric cancer progression by stabilizing BMI1 protein. *Oncotarget*. (2017) 8:33329–42. doi: 10.18632/oncotarget.16445

24. Xiong W, Xu H, Li Y, Wang Y, He L. RNF220 enhances USP22 to promote cell growth, metastasis and stemness in hepatocellular carcinoma by activating the Akt pathway. *Cell Cycle*. (2025) 24:316–28. doi: 10.1080/15384101.2025.2550448

25. Zhao X, He X, Wei W, Huang K. USP22 aggravated diabetic renal tubulointerstitial fibrosis progression through deubiquitinating and stabilizing Snail1. *Eur J Pharmacol*. (2023) 947:175671. doi: 10.1016/j.ejphar.2023.175671

26. Lange SM, Armstrong LA, Kulathu Y. Deubiquitinases: From mechanisms to their inhibition by small molecules. *Mol Cell*. (2022) 82:15–29. doi: 10.1016/j.molcel.2021.10.027

27. Deng Z, Siraj AA, Lowry I, Ruan E, Patel R, Gao W, et al. Nanoparticle-based delivery systems for synergistic therapy in lung cancers. *Bioengineering (Basel)*. (2025) 12:968. doi: 10.3390/bioengineering12090968

28. Zhang XY, Varthi M, Sykes SM, Phillips C, Warzecha C, Zhu W, et al. The putative cancer stem cell marker USP22 is a subunit of the human SAGA complex required for activated transcription and cell-cycle progression. *Mol Cell*. (2008) 29:102–11. doi: 10.1016/j.molcel.2007.12.015

29. Di Q, Zhao X, Tang H, Li X, Xiao Y, Wu H, et al. USP22 suppresses the NLRP3 inflammasome by degrading NLRP3 via ATG5-dependent autophagy. *Autophagy*. (2023) 19:873–85. doi: 10.1080/15548627.2022.2107314